This article has been accepted for inclusion in a future issue of this journal. Content is final as presented, with the exception of pagination.
IEEE JOURNAL OF SOLID-STATE CIRCUITS

Enhanced-Selectivity High-Linearity Low-Noise Mixer-First Receiver with Complex Pole Pair due to Capacitive Positive Feedback

Yuan-Ching Lien, *Member, IEEE*, Eric Klumperink, *Senior Member, IEEE*, Bernard Tenbroek, Jon Strange, *Senior Member, IEEE*, Bram Nauta, *Fellow, IEEE*

***Abstract*— A mixer-first receiver with enhanced selectivity and high dynamic range is proposed, targeting to remove SAW-filters in mobile phones and cover all frequency bands up to 6 GHz. Capacitive negative feedback across the baseband amplifier serves as a blocker bypassing path, while an extra capacitive positive feedback path offers further blocker rejection. This combination of feedback paths synthesizes a complex pole pair at the input of the baseband amplifier, which is up-converted to the RF port to obtain steeper RF-bandpass filter roll-off and reduced distortion. This paper explains the circuit principle and analyzes receiver performance. A prototype chip fabricated in 45nm Partially Depleted SOI technology achieves high out-of-band linearity (IIP3=39 dBm, IIP2=88 dB) combined with sub-3 dB noise figure. Desensitization due to a 0-dBm blocker is only 2.2 dB at 1.4 GHz.**

***Index Terms*— receiver, mixer-first, N-path filter, bandpass, tunable, passive mixer, block rejection, SAW-less, FDD, wideband, CMOS, high linearity, low noise, IIP3, IIP2, compression point.**

I. INTRODUCTION

To improve data rate and capacity, cellular phones based on the long-term evolution (LTE) standard have to support an ever increasing number of bands. For 5G, a receiver (RX) covering much of the spectrum up to 6 GHz is likely required. The mobile receivers need to deal with large out-of-band (OOB) blockers, while Frequency Division Duplex (FDD) also introduces strong self-interference from the transmitter (TX). To prevent degradation in sensitivity, off-chip high-linearity surface acoustic-wave (SAW) filters are often adopted. However, these filters are not tunable, increase size and cost, and introduce 2-3 dB in-band loss, making multi-band 1-6 GHz support troublesome. SAW-less solutions compatible with CMOS integration are highly desired.

Antenna diversity with two antennas is widely applied in modern cellular phones to improve the quality and reliability of wireless links. Moreover, two or even more receive antennas are wanted for MIMO. In this paper we focus on a diversity antenna receiver for a conventional FDD cellular system as shown in Fig. 1(a).

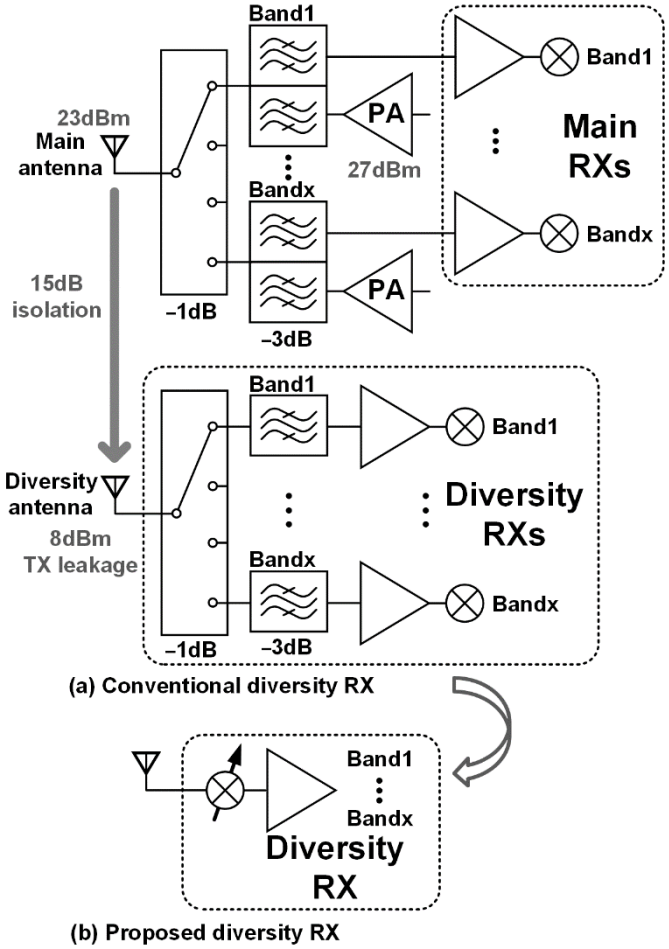

Fig. 1. (a) Conventional LTE receiver with external SAW filters. (b) proposed single tunable diversity receiver without external SAW filters.

The typical TX-power is as strong as +27 dBm and there is about 15 dB isolation from the main antenna to the diversity antenna. Including TX-filter and switch losses, about +23 dBm and +8 dBm TX-leakage are present at the RF input ports of the main and diversity receivers respectively. Usually SAW RX-filters (see Fig. 1(a)) provide TX-RX isolation to relax the RX-

This paragraph of the first footnote will contain the date on which you submitted your paper for review. It will also contain support information, including sponsor and financial support acknowledgment. For example, "This work was supported/funded by Mediatek.

The next few paragraphs should contain the authors' current affiliations, including current address and e-mail. For example, F. A. Author is with the National Institute of Standards and Technology, Boulder, CO 80305 USA (e-mail: author@ boulder.nist.gov).

linearity requirements to a feasible level. Targeting more integration, recent work shows that passive switch-capacitor N-path filtering with tunable center frequency in mixer-first receivers can achieve >10 dBm blocker 1-dB compression point (B1dB) and good IIP3 of 20-30 dBm [1-3]. This shows promise to remove the off-chip SAW filters in the diversity receiver and also reduce the number of diversity receivers to a single one, as shown in Fig. 1(b). This paper explores the feasibility of such a receiver in CMOS.

In a FDD system, cross-modulation due to TX leakage and an in-band continuous-wave (CW) blocker deteriorates RX sensitivity, which can be related to an IIP3 requirement [4, 5]:

$$\mathrm{IIP3} = \frac{P_{\mathrm{cw}} + 2P_{\mathrm{TX}} - P_{\mathrm{XM}} - 5}{2} \qquad (1)$$

As shown in Fig. 2(a), P_{cw} is the power of the CW blocker (typically −40 dBm), P_{TX} that of the TX leakage (8 dBm), P_{XM} the power of the cross-modulation product, while the last term (=5 dB) is added to account for the modulated nature of the TX [4]. For example, the integrated thermal noise is −101 dBm for 20-MHz channel BW in an LTE receiver. If we assume the cross-modulation product is equal to the noise power, i.e. $P_{\mathrm{XM}} = -101$ dBm, the resulting required IIP3 is +36 dBm, which is a challenging specification that we will try to meet.

Figure 2(b) shows some examples of LTE frequency bands. A single switch-R-C N-path filter [6] or mixer-first receiver [1] performs "only" 1st order Low Pass Filtering (LPF), which is up-converted to a 2nd order Band-Pass Filter (BPF) around the switching frequency. However, this is not sufficient to deal with strong TX-leakage in case of a very small "duplex spacing" (e.g. band 5 and 8 in Fig. 2(b)).

To enhance the selectivity and extend the linearity, a 6th order BPF was realized by cascading passive N-path filters, coupling them by transconductors g_{m} [7]. These transconductors work at RF in open loop and have a rather limited achievable linearity of around 10-15 dBm [8]. Even with a first passive stage [7], overall linearity was limited to +25 dBm, which is >10 dB worse than the +36 dBm requirement. Also, other g_{m}−C filter techniques, e.g. [9] achieve good selectivity but insufficient linearity. An IIP3=36 dBm was demonstrated by [5], however at boosted switch-driver supply voltage of 2 V, raising power dissipation, and introducing device reliability concerns. Recently, we proposed higher order RF filtering by cascading two passive BPF stages [10], while a "Bottom-plate mixing" technique with switch sharing pushes IIP3 to +44 dBm. Unfortunately, large parasitic capacitance from MOM capacitors at the RF input introduce signal loss, and sub-3dB noise figure (NF) was not obtained.

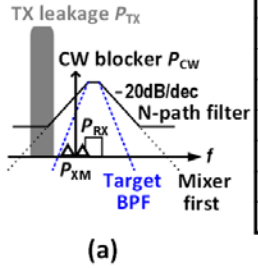

Band	f_{TX} (MHz)	f_{RX} (MHz)	Duplex Spacing (MHz)
1	1920 – 1980	2110 – 2170	190
2	1850 – 1910	1930 – 1990	80
3	1710 – 1785	1805 – 1880	95
5	824 – 849	869 – 894	45
7	2500 – 2570	2620 – 2690	120
8	880 – 915	925 – 960	45
22	3410 – 3490	3510 – 3590	100

(b)

Fig. 2. (a) The related target-BPF profile and (b) some LTE frequency bands.

In this paper we propose a different approach to enhance selectivity in a mixer-first receiver: we will exploit capacitive positive feedback to obtain a steeper filter roll-off [11], increased frequency range and enhanced linearity, while achieving a noise figure below 3 dB. Note that this is different from [3], where positive resistive (not capacitive) feedback is added to aid input impedance matching and realize sub 3-dB NF, whereas our key target is selectivity enhancement at high linearity. Compared to [11], this paper explains the concept in more depth, analyzes the filter transfer, noise figure and stability, and adds some extra experimental results.

This paper is organized as follows. Section II introduces the architecture of the enhanced-selectivity mixer-first receiver, while section III proposes a circuit implementation. In Section IV the receiver performance is analyzed, especially transfer function, loop stability, distortion, noise and input impedance. Section V shows the measurement results and a performance comparison, while Section VI provides conclusions.

II. RECEIVER ARCHITECTURE

To enhance IIP3 and compression point of the entire receiver, strong OOB signals should be rejected as early as possible by steep filtering. This is what a SAW filter does, immediately at the RF-input, but as motivated in the introduction we would like a more CMOS compatible solution exploiting N-path filtering.

Figure 3(a) shows a mixer-first receiver, in which capacitor C_1 is put across negative feedback amplifier $-A_0$ and interacts with source impedance R_s via a passive mixer to obtain N-path filtering[1-3, 11-13]. The resulting first order low-pass filter is frequency shifted to a 2nd order RF bandpass filter around f_{LO}. By putting C_1 across the amplifier instead of to ground, the baseband (BB) capacitance "seen" by the mixer is increased due to the Miller effect by $(1 + A_0)$, saving chip area. Moreover, this Miller effect allows for low-noise impedance matching using a high R_{F} value [1]. A single-stage amplifier will be used, modelled as a voltage controlled current source g_{m} with output resistance r_{o}, where $A_0 = g_{\mathrm{m}} r_{\mathrm{o}}$. Assuming $r_{\mathrm{o}} \ll R_{\mathrm{F}}$, an OOB blocker is down-converted and sees a baseband conductance

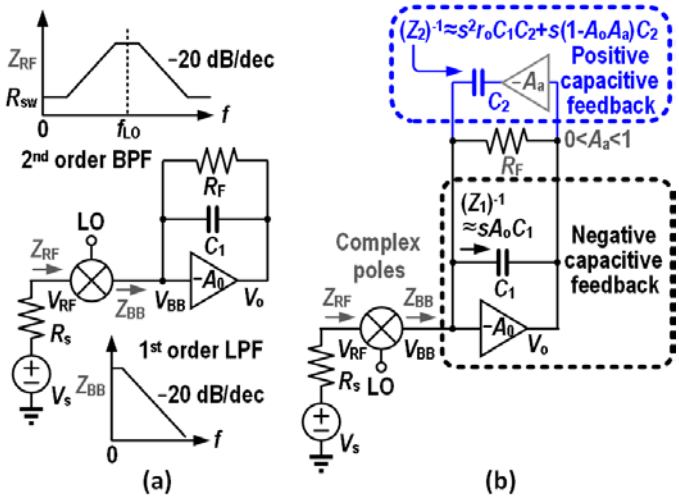

Fig. 3. (a) Mixer-first receiver with the BB Miller capacitor C_1; (b) The proposed receiver with extra positive capacitive feedback.

$(Z_{BB})^{-1} \approx (Z_1)^{-1} + (1+A_0)/R_F$, with $(Z_1)^{-1} \approx s(1+A_o)C_1/(1+sr_oC_1)$. For frequencies $\ll (r_oC_1)^{-1}$ and $A_o \gg 1$, conductance $(Z_1)^{-1} \approx sA_oC_1$ offers OOB current by-passing and first order filtering.

Higher order filtering can be obtained by creating a higher order input conductance as shown in Fig. 3(b). A capacitive positive feedback path is added in the form of capacitor C_2, driven by the attenuated inverted BB signal, rendering:

$$(Z_2)^{-1} \approx \frac{[s^2 r_o C_1 C_2 + s(1-A_0A_a)C_2]}{1+sr_oC_1} \quad (2)$$

where A_0 and A_a are positive numbers. The combination of negative feedback via C_1 and positive feedback via C_2 produces a 2-zero, 1-pole conductance, which can be approximated as:

$$(Z_2)^{-1} + (Z_1)^{-1} \approx \frac{[s^2 r_o C_1 C_2 + s(1-A_0A_a)C_2 + sA_0C_1]}{1+sr_oC_1} \quad (3)$$

By choosing a proper A_a and C_1/C_2 ratio, both zeros in (3) can be located at a frequency lower than $(r_oC_1)^{-1}$, and the conductance for a blocker offset frequency $< (r_oC_1)^{-1}$ can be approximated as $s^2 r_o C_1 C_2 + s(1-A_0A_a)C_2 + sA_0C_1$. This gives the approximations $(Z_2)^{-1} \approx s^2 r_o C_1 C_2 + s(1-A_0A_a)C_2$ and $(Z_1)^{-1} \approx sA_0C_1$ as shown in Fig. 3(b).

To get more detailed insights into the proposed mixer-first RX, we assume that 4 BB-slices of the circuit of Fig. 3(b) are driven by 4 mixers and non-overlapping 4-phase clocks with 25% duty-cycle. The 4-phase example of proposed RX is shown in Fig. 4(a). We still assume that A_a is an ideal attenuator with infinite input impedance and zero output impedance. Adopting a derivation as in [14], we derived an equivalent Linear Time Invariant (LTI) model of the time variant circuit and voltage transfer functions from the RF signal V_s to the BB. The resulting LTI model for a sinewave RF-excitation is shown in Fig. 4(b) (note that the left part of the circuit operates at RF, and the right part at $\omega_{BB} = \omega_{RF} - \omega_{LO}$ as in [14]). The harmonic shunt impedance R_{sh} of the passive mixer is $4\gamma R_s/(1-4\gamma)$ [15]. Assuming ideal mixer switches, the voltage gain from V_{RF} to V_{BB} can be derived by dividing Eqn. 4 in [15] by Eqn. 6, resulting $1/\sqrt{4\gamma}$ (=0.9 dB) where γ is $2/\pi^2$ for 4-phase case. In our RX design, r_o is small because a large g_m is required for low noise. R_F is much higher than R_s, because $R_F \approx R_s(1+A_0)/(8\gamma-1)$ is needed for input matching. We first show the single-ended to single-ended voltage transfer function $H_{BB,S}(s) = V_{BB}(s)/(V_s/2)$, and its natural frequency $\omega_{0,S}$ and quality factor Q_S:

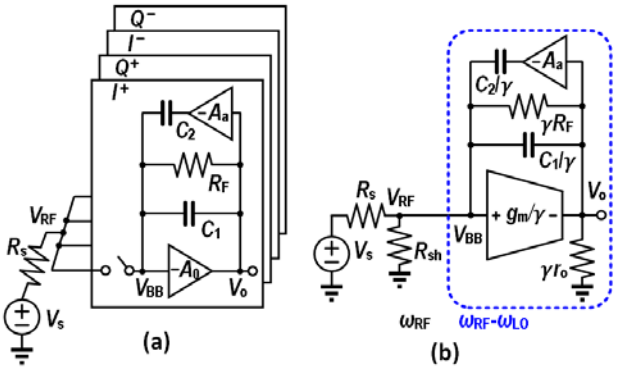

Fig. 4. (a) A 4-phase case of the proposed receiver and (b) the corresponding LTI model.

$$H_{BB,S}(s) = \frac{V_{BB}(s)}{V_s/2} \approx \frac{2\sqrt{4\gamma}((1+A_a)C_2 4R_s)^{-1}(s+1/(r_oC_1))}{s^2 + \frac{\omega_{0,S}}{Q_S}s + \omega_{0,S}^2} \quad (4)$$

$$\omega_{0,S} \approx \sqrt{\frac{1+4g_m r_o R_s R_F^{-1}}{4(1+A_a)C_1C_2r_oR_s}} \quad (5)$$

$$Q_S \approx \frac{2\sqrt{(1+A_a)C_1C_2r_oR_s(1+4g_m r_o R_s R_F^{-1})}}{4C_2(1-A_a g_m r_o)R_s + C_1(r_o + 4R_s + 4g_m r_o R_s)} \quad (6)$$

When $\omega_{BB} < 1/(r_oC_1)$, $V_{BB}(s)/(V_s/2)$ is a LPF with 2-pole roll-off. As ω_{BB} increases to $1/(r_oC_1)$, this unwanted zero is introduced because Miller capacitor C_1 is no longer valid.

Next, we derive the $H_{o,S}(s) = V_o(s)/(V_s/2)$, and it can be written as:

$$H_{o,S}(s) = \frac{V_o(s)}{V_s/2} \approx \frac{2\sqrt{4\gamma}((1+A_a)C_2 4R_s)^{-1}(s-g_m/C_1)}{s^2 + \frac{\omega_{0,S}}{Q_S}s + \omega_{0,S}^2} \quad (7)$$

The frequency of unwanted zero in $H_{o,S}(s)$ that is located at g_m/C_1 can be as high as 1 GHz if g_m is large enough. Then $H_{o,S}(s)$ effectively shows a 2-pole roll-off below g_m/C_1. Fig. 5 compares the filter shape of a 4-phase mixer-first receiver with a BB Miller capacitor C_1 in Fig. 3(a) and that of the new one with C_1 and C_2 in Fig. 3(b), designed as Butterworth filter. Clearly, a more brick-wall like and also steeper RF BPF-shape and BB LPF-shape is achieved for blocker frequencies close to the RX band compared to the "round shape" when cascading real poles.

We see that the combination of the new positive feedback path via C_2 combined with the negative feedback path via C_1 can establish a complex pole-pair allowing to improve selectivity.

The quality factor Q is adjustable by changing the ratio of C_1 and C_2. Note that both BB capacitive feedback paths can have *high linearity as well as low noise, in contrast to open loop g_m blocks*. Before we analyze the practical circuit with *non-ideal attenuator* A_a in depth, we describe the actual circuit implementation in some more detail.

III. CIRCUIT IMPLEMENTATION

Figure 6 shows a detailed schematic of the proposed zero-IF receiver. It was designed for $f_{-3dB,BB}$=10 MHz to support an

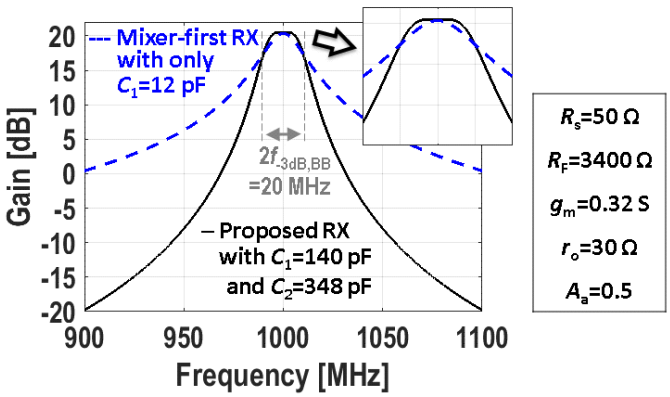

Fig. 5. Simulated (PXF) $V_o(s)/(V_s/2)$ for the mixer-first RX with only C_1 (dashed line) and the proposed mixer-first RX with C_1 and C_2 (solid line). C_1 and C_2 are tuned to have the same channel BW for fair comparison.

RF channel bandwidth of 20 MHz for LTE applications. The passive mixer MOS-switches are driven by quadrature 4-phase 25% duty-cycle clocks, provided by a divide-by-2 circuit. Parasitic capacitance at the RF input causes the frequency of optimum S_{11} to shift towards lower frequencies than f_{LO}, which was compensated by complex feedback via R_{FIQ} [1].

A. Enhanced selectivity receiver circuit realization

Due to the differential architecture, the negative gain $-A_a$ for the attenuator in Fig. 6 can simply be implemented by wire-crossing, while low-ohmic passive resistors R_{a1} and R_{a2} realize a high-linearity attenuator with $A_a = 0.5$. In section IV we will see that this hardly degrades NF. As C_2 serves as OOB blocker bypassing path, low OOB impedance of the attenuator is important to maintain good blocker rejection. For this purpose capacitor C_a is added, providing a high linearity purely capacitive signal path shunting the BB-input directly (see Fig. 6). The filter bandwidth is mainly determined by R_s, C_1 and C_2, as will be derived in section IV, and Q is designed about 0.7 to realize Butterworth filtering. Capacitor C_B also provides a direct blocker bypassing path to ground but plays a minor role in this design, as the TIA-input impedance is low-ohmic over a wide band due to the high g_m value used in this design (see below).

B. Low noise BB amplifier

In the mixer-first receiver, low noise in the first BB amplifier stage is an important requirement to achieve sub-3dB receiver NF. Inverter-based amplifiers [16, 17] offer large g_m with good power efficiency, while loop stability is of little concern in a single-stage amplifier. Figure 6 shows the schematic of the BB amplifier also used in [10]. A higher threshold voltage V_{th} for M_{cm1} and M_{cm2}, combined with a small overdrive voltage of the PMOS input differential pair ensures all transistors operate in their saturation region. The resistive attenuator in parallel to the MOS output resistance r_{on} and r_{op} linearizes the output impedance of the BB amplifier. For a differential input signal, a high gain of $\approx (g_{mn} + g_{mp})(r_{on}\|r_{op})$≈22 dB is achieved. For a pure common mode input, the voltage-gain g_{mn}/g_{mcm} is kept low as 5 dB. To avoid the kink or history effect in partially depleted SOI-MOS transistors [18], the BB amplifiers were built by body contacted devices, while mixer switches and digital clock generator devices are implemented as floating body devices. The dimensions of PMOS and NMOS input pairs are 3600 um/0.112 um and 1600 um/0.112 um respectively, achieving a large g_m of 360 mS and an output impedance $r_o = r_{on}\|r_{op}$=36 Ω. The simulated flicker noise corner frequency is about 50 kHz, and the open loop bandwidth is about 340 MHz for a 10-pF loading capacitance.

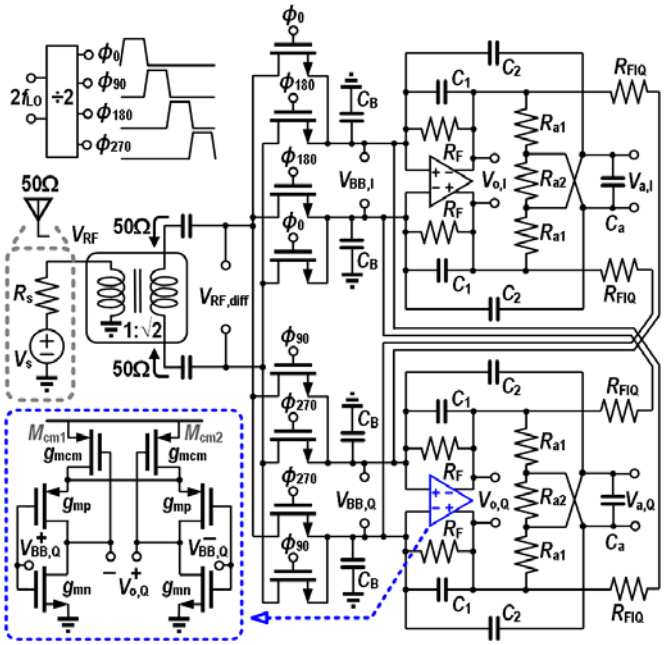

Fig. 6. Circuit details of the proposed receiver and low noise BB amplifier.

IV. CIRCUIT ANALYSIS

In this section we will analyze different properties of the mixer-first receiver, like transfer function, loop stability, linearity, noise and input impedance.

A. Transfer function analysis

Using a similar derivation as in [14], we derived voltage transfer functions from V_s to $V_{BB,diff}$, $V_{o,diff}$ and $V_{a,diff}$ in Fig. 7. However, in contrast to a single balanced mixer, we use a double-balanced mixer. Now each of the baseband components is connected twice per period to the RF source, doubling the conduction time, compared to the single-end case. This leads to an equivalent LTI model with extra factors 2 as given in Fig. 7(a). The transformer with 1:n turns ratio performs single to differential conversion. In this design, it is n=$\sqrt{2}$ and impedance ration is 1:2. To reduce equation complexity, we assume $2R_{a1} = R_{a2} = R_a$ and neglect the minor effect of C_B. The pole and zero located at frequency higher than 500 MHz are also neglected. We derived $H_o(s) = V_{o,diff}(s)/(V_s/2)$, its natural frequency ω_0 of the pole-pair and quality factor Q as shown in Eqn. (8-10). Since we consider now the finite gain of the BB amplifier, the equation becomes more complex than a normal biquad transfer function. The resistive attenuator A_a instead of the uni-lateral block $-A_a$ induces an unwanted left half s-plane zero located at $(0.5R_aC_a)^{-1}$. It can be moved to higher frequency by using smaller attenuator resistance or C_a.

$$H_o(s) = \frac{V_{o,diff}(s)}{V_s/2} \approx -2\sqrt{2}\sqrt{4\gamma}\,\frac{2R_F/(1+g_m(r_o^{-1}+R_a^{-1}+R_F^{-1})^{-1})}{4R_s+2R_F/(1+g_m(r_o^{-1}+R_a^{-1}+R_F^{-1})^{-1})}\,\frac{g_m(r_o^{-1}+R_a^{-1}+R_F^{-1})^{-1}\omega_0^2(0.5R_aC_as+1)}{s^2+\frac{\omega_0}{Q}s+\omega_0^2} \quad (8)$$

$$\omega_0^2 \approx \frac{2(r_o(R_F+2R_s)+R_a(R_F+r_o+2R_s+2g_mr_oR_s))}{R_a(C_2C_a(2R_Fr_o+R_a(R_F+r_o))2R_s+C_1R_F(6C_2r_oR_s+C_a(4r_oR_s+R_a(r_o+2R_s+2g_mr_oR_s))))} \quad (9)$$

$$Q \approx \frac{\sqrt{(r_oR_F+R_a(R_F+2g_mr_oR_s))2R_a\left(C_2C_a(2R_Fr_o+R_aR_F)2R_s+C_1R_F(6C_2r_oR_s+4C_ar_oR_s+2C_aR_ag_mr_oR_s)\right)}}{C_2(3R_ar_o+2R_Fr_o+R_aR_F(2-g_mr_o))2R_s+2C_1R_F(2r_oR_s+R_a(r_o+2R_s+2g_mr_oR_s))+C_aR_a(2r_oR_F+R_a(R_F+2g_mr_oR_s))} \quad (10)$$

Filling in the component values listed in TABLE I, we find: $\omega_0/2\pi$ =9.5 MHz, and a zero at 31 MHz. At ω_0, the amplitude of $H_o(s)$ is $Q \cdot V_{o,diff}(0)/(V_s/2)$ so for a Butterworth filter $Q \approx 0.7$, $\omega_0 = \omega_{BB,-3dB}$. The simplified asymptotic plots of the transfer function to $V_{RF,diff}$, $V_{BB,diff}$ and $V_{o,diff}$ are shown in Fig. 7(b). The BB resistance $R_F/(1+A)$ is up-converted and becomes $2\gamma R_F/(1+A)$ at the RF input, where $\gamma = 2/\pi^2$ for the 4-path case [15] and A is $g_m(r_o||R_a||R_F)$. The up-converted BB resistance is in parallel with the harmonic shunt impedance $R_{sh} = (0.5n^2R_s)4\gamma/(1-4\gamma)$ of the passive mixer [15], where n is turns ratio of the transformer. The combined input impedance around the LO frequency is $R_{sh}||2\gamma R_F/(1+A)$ which is designed to provide 50-ohm matching. If there is in-band matching, in-band $V_{RF}/(V_s/2)$ is 0 dB. Due to energy conservation, $V_{RF,diff}/V_{RF}$ after the 1:$\sqrt{2}$ balun (100-Ω differentially) becomes +3 dB. The in-band voltage gain $V_{BB,diff}/V_{RF}$ is $\sqrt{2}(\sqrt{4\gamma})^{-1}$ corresponding to 3.9 dB. At the output of the BB amplifier $V_{o,diff}$, it is 3.9+20$logA$ dB. For frequencies close to in-band, the roll-off is −12 dB/octave. The output RC of the attenuator introduces a zero at 31 MHz and hence the slope degrades to −6 dB/octave far out. Still, this steep roll-off part allows for better selectivity close to the desired band. Compared to the mixer-first receiver with only Miller capacitor C_1, simulations indeed show about 10 dB improvement in OOB IIP3 for the same mixer switch size, channel bandwidth and BB amplifier gain.

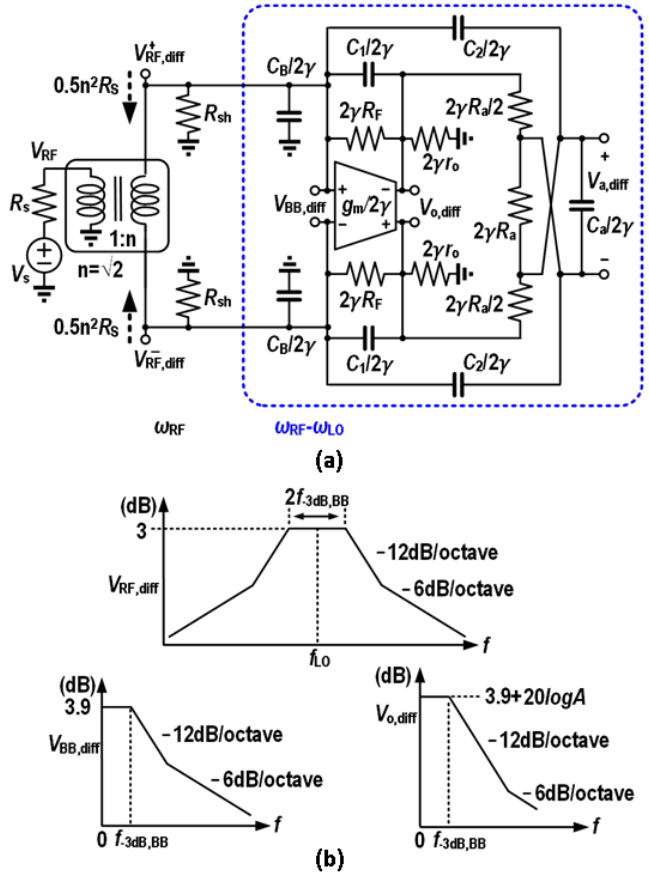

Fig. 7. (a) Equivalent LTI model of this receiver, (b) simplified plots for $V_{RF,diff}$, $V_{BB,diff}$ and $V_{o,diff}$.

TABLE I
COMPONENT VALUES FOR FIG. 7

C_1=60 pF	C_a=120 pF	R_F=1600 Ω	r_o=36 Ω
C_2=106 pF	C_B=20 pF	R_a=90 Ω	g_m=0.36 S

The IIP3 simulation results with transistor level BSIM models are provided in Fig. 8(b) to demonstrate that the extra filtering also results in extra overall IIP3 improvement. Since we experienced convergence issues using PSS simulations and there are effects of the discontinuity in the BSIM model, transient simulations with high accuracy settings and sufficiently high input power (−10 dBm to +5 dBm) were applied to evaluate the IIP3. Intuitively this makes sense, as the part of the waveform defined by the discontinuity becomes a smaller fraction of the total waveform. Overall, we found then a reasonable match (within 2-3 dB difference) between simulation and measurement.

The process, voltage and temperature (PVT) variation simulation results for transfer function, NF and IIP3 are shown in Fig. 9. The BPF bandwidth or ω_0 is controlled by RC value. The ''filter shape'' is determined by quality factor Q which is a function of R-to-R and C-to-C ratios, hence it is insensitive to PVT variations. The frequency axis of Fig. 9(a) is shifted to BB frequency and normalized to $f_{-3dB,BB}$. The RX transfer functions are redrawn and shown in Fig. 9(b) to confirm the robustness of RX selectivity against PVT variations. The simulated IIP3 as a function of relative frequency offset in Fig. 9(c) is kept within ≈3 dB variations while compared to the typical corner.

B. Receiver loop stability

Positive feedback may introduce stability problems, so we will now analyse the feedback system loop gain $H_{l,diff}(s)$, i.e.:

$$H_{l,diff}(s) = [-A(s)] \cdot [-A_a(s)] \cdot \beta(s) \qquad (11)$$

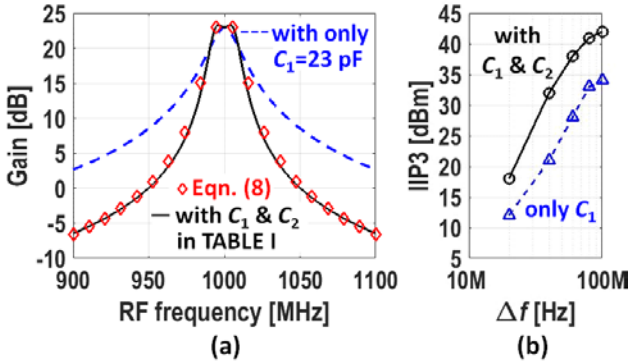

Fig. 8. (a) Simulated (PXF) and calculated (Eqn. (8)) gain ($V_{o,diff}(0)/(V_s/2)$) as a function of the RF frequency for the proposed mixer-first RX with C_1 and C_2 (solid line) and with only C_1 (dashed line). (b) IIP3 simulation result for the same two cases.

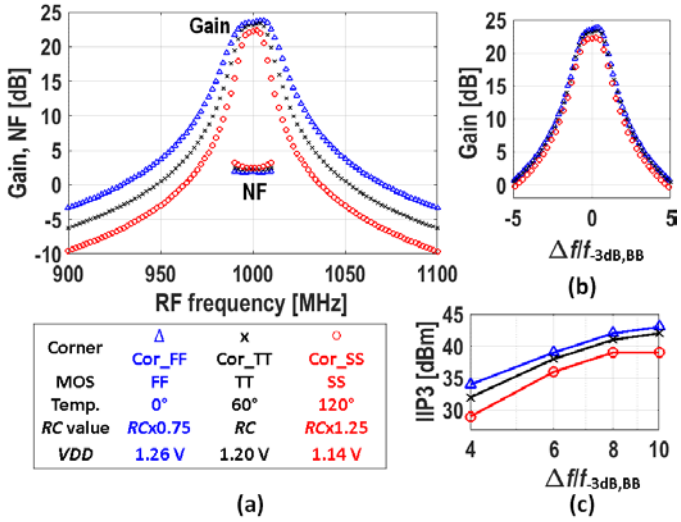

Fig. 9. The PVT corner simulation results for (a) transfer function $V_{o,diff}(0)/(V_s/2)$, NF, (b) redrawn transfer function as a function of normalized frequency axis and (c) IIP3.

As the resistance of the attenuator is higher than r_o, the gain of the amplifier can be approximated as $A(s)\approx A_0/(1+sr_oC_1)$. The frequency dependent gain of attenuator can be approximated as $A_a(s) \approx A_a/(1+s(R_{a1}||0.5R_{a2})(2C_a+C_2))$. It is a low pass function and $A_a = 1/2$. Applying the Miller approximation, the feedback factor from attenuator output to the BB amplifier input is $\beta(s) \approx s(C_2/C_1)/((R_s||(A_0^{-1}R_F)C_1)^{-1}+s(C_2/C_1+1+A_0))$, which is a high-pass function. The positive loop gain $H_{l,diff}(s)$ should be kept well below 0 dB to guarantee loop stability. At very low frequency, C_2 provides a high impedance and $\beta(0)\approx 0$, so that $H_{l,diff}(0)\approx 0$. For increasing frequency, the impedance of C_1 and C_2 becomes lower resulting in lower $A_0(s)$ and lower $A_a(s)$ but higher $\beta(s)$. In this receiver design, $C_2\approx 2C_1$, resulting in $H_{l,diff}(s) < A_0A_a(C_2/C_1)/(C_2/C_1+1+A_0) = A_0/(3+A_0) <$ 1 for all frequencies. The resistive attenuator occupies a rather large area of 20 um x 40 um to prevent linearity degradation due to the voltage coefficient of poly resistors, which also results in a good matching and an accurate resistor ratio A_a. Capacitance C_1 and C_2 are large, so C_2/C_1 is also precise. The open loop gain of the BB amplifier A_0 suffers more from process variation, but largely cancels in the ratio $A_0/(3+A_0)$ and reliably gives a value below 1. Therefore loop stability is insensitive to PVT variations. Transistor-level Spectre PSS PSTB loop stability simulation shows $H_{l,diff}(s)$ is <–6 dB for different transistor, *R*, *C*, voltage and temperature corners. The antenna impedance may change with user proximity in a mobile phone and the antenna impedance Z_s may become more resistive and inductive [19]. Further analysis indicates that the proposed receiver remains stable for different passive complex values of Z_s. As shown in Fig. 10, the simulated differential loop gain shows a BPF profile as predicted in (11), and is kept well below –4 dB (<0 dB for stable) for all frequencies even though there is 10x Z_s variation. For common mode signals, the wire-crossing no longer results in a minus sign, and it becomes positive and unity gain. As a result, equation (11) changes to:

$$H_{l,CM}(s) \approx \frac{-A_{0,CM}}{1+sr_oC_1}\frac{sC_2/C_1}{((R_s||(A_0^{-1}R_F)C_1)^{-1}+s(C_2/C_1+1+A_0))} \quad (12)$$

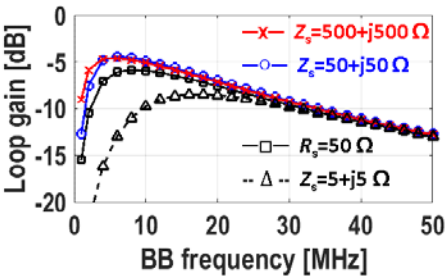

Fig. 10. Simulated differential loop gain for different antenna impedance Z_s.

Hence the common mode loop gain $H_{l,CM}(s)$ turns out to be negative feedback, in contrast to the differential loop gain $H_{l,diff}(s)$. Also the single stage BB amplifier (single pole) is designed to have a low common-mode gain resulting in $|H_{l,CM}(s)| < 1$. Hence, there is no common-mode loop stability concern.

C. OOB linearity and OOB rejection

The NMOS mixer switches suffer from modulated V_{GS} and V_{DS} that degrade the linearity of a mixer-first receiver. Assuming $\rho = R_{sw}/R_s << 1$ (e.g. $\rho < 0.1$) to achieve high linearity, in-band matching is mainly realized by R_F. For in-band, the V_{GS} modulation is $\approx 0.5V_A$ and V_{DS} modulation is $\approx 0.5V_AR_{sw}/R_s$ where V_A is the amplitude of the antenna source voltage. The in-band linearity of a mixer is dominated by large V_{GS} modulation. When the blocker offset frequency from the LO increases, V_{GS} modulation is reduced due to filtering. But V_{DS} modulation is slightly increased as the OOB current is higher than in-band. When the blocker is very far away from the LO frequency, the source terminal voltage swing of the mixer switch becomes almost zero, i.e. V_{GS} modulation ≈0. The modulated V_{DS} is $\approx V_AR_{sw}/R_s$ and dominates the OOB linearity. The far OOB IIP3 can be estimated as [14]:

$$V_{IIP3} = \sqrt{\frac{4}{3}\frac{(1+\rho)^4}{\rho^3(2g_2^2-g_3(1+\rho))}} \quad (13)$$

Where g_2 is $-(2V_{OD})^{-1}$ and $g_3 = -(2V_{SAT}^2)^{-1}$. V_{OD} is overdrive voltage and V_{SAT} is velocity saturation voltage respectively [14]. When the blockers are close to the LO frequency, the proposed mixer-first receiver with enhanced RF selectivity achieves better OOB rejection and better linearity as the simulation results in Fig. 8 show.

To obtain extremely high OOB IIP3 of almost +40 dBm, high OOB linearity as well as high OOB rejection for both the mixer and the low noise BB amplifiers are demanded. The maximum OOB rejection of a mixer-first receiver with a BB Miller capacitor that is shown in Fig. 3(a) is limited to $\approx g_m^{-1}/R_s$ at the input of the BB amplifier. The OOB rejection can be extended by adding a capacitor C_B to ground [1, 13]. However, for the same BW a much larger capacitance area is required compared to C_1. Normally, there is a design trade-off between linearity and maximum OOB rejection. The gain of the BB amplifier as a function of frequency can be expressed as $A_o/(1+A_o\beta(s))$. The Miller capacitor C_1 across the amplifier increases the feedback factor $\beta(s)$ and improves the linearity of the BB amplifier at higher frequencies [20], while a BB

amplifier without Miller capacitor becomes linearity constraint in [13]. A high supply voltage of the BB amplifier can also result in better linearity [1], but consumes more power. Apart from the linearizing effect of the Miller capacitance, the output impedance of the BB amplifier is linearized by shunting it with the resistive attenuator. By adding C_a we also directly shunt the BB amplifier input, avoiding the limited OOB rejection due to the finite g_m of BB amplifier. In the proposed mixer-first receiver design, the maximum OOB rejection of the BB amplifier is improved compared to the mixer-first RX with BB Miller capacitors in Fig. 3(a) and the linearity of the BB amplifier is improved compared to [1, 13].

D. Noise performance

The noise factor F of the receiver can be calculated as the total output noise divided by the noise contribution due to the thermal noise from the antenna or signal source, modelled as $\overline{v_{n,s}^2} = 4kTR_s$. The resulting F of this RX can be written as:

$$F = 1 + \frac{R_{sw}}{R_s} + \frac{(R_s+R_{sw})}{4.3R_s} + \frac{(R_s+R_{sw})^2}{\gamma(2R_F)R_s} + \frac{\overline{v_{n,in,A}^2}(4(R_s+R_{sw})+2R_{BB})^2}{4kTR_s4\gamma(2R_{BB})^2} + \frac{(r_o||R_a)^2(4(R_s+R_{sw})+2R_{BB})^2}{A^2R_aR_s4\gamma(2R_{BB})^2} \quad (14)$$

The direct noise contribution from thermal noise of the mixer switch resistance which is in series with the source is R_{sw}/R_s. Moreover, noise degradation due to noise folding from odd harmonics of the mixer frequency occurs. Thermal noise of R_s and R_{sw} are hence down converted [15], leading to a summation of $4kT(R_s + R_{sw})/n^2$ terms, where $n = 3, 5, 7, \ldots$ for a 4-path mixer. This sums up to $\approx 4kT(R_s + R_{sw})/4.3$. The up-converted noise current induced by the BB feedback resistor R_F renders the term proportional to $1/(2\gamma R_F)$, where γ is the scaling factor from [15] discussed in sub-section A. Note that R_F is designed to provide 50 ohm matching, but it is much higher than R_s primarily due to the Miller effect. Therefore the noise contribution of R_F is minor and it increases F by about only 0.08 in this design. The input-referred noise of the BB amplifiers $\overline{v_{n,in,A}^2}$ is $\overline{v_{n,out,A}^2}/A^2$, where $A = g_m(r_o||R_a||R_F)$ and $\overline{v_{n,out,A}^2}$ is noise at the BB amplifier output. The noise voltage due to source resistance at the BB amplifier input undergoes a voltage division with gain of $\sqrt{4\gamma}$ and it is $\overline{v_{n,s,BB}^2} = 4kTR_s(4\gamma)(2R_{BB}/(4(R_s + R_{sw}) + 2R_{BB}))^2$, where R_{BB} is $R_F/(1 + A)$. The BB amplifier generates $\sqrt{(\overline{v_{n,out,A}^2})} = 1400\ pV/\sqrt{Hz}$, and the $\overline{v_{n,in,A}^2}/\overline{v_{n,s,BB}^2}$ is low as 0.1 in this design. The last term in Eqn. (14) comes from the resistive attenuator. The noise voltage is $\overline{v_{n,att}^2} = 4kT(r_o||R_a)^2/R_a$ where r_o is the output impedance of the MOS transistors. This contribution to F is only 0.006.

Equation (14) indicates that this RX design can achieve a NF of 1.6 dB ($F = 1.46$) at low frequency with $R_{sw} = 1.1\ \Omega$, where the harmonic folding term is the dominant one.

E. Influence of parasitic capacitance at the RF input port

In a mixer-first receiver or N-path filter, the optimum S_{11} (dip in S_{11}) should be at ω_{LO}. However, the parasitic capacitance C_p from the mixer switches, RF input pads and tracks is in parallel with $R_{in}(\omega_{LO}) = R_{sh}(\omega_{LO})||(\gamma 2R_{BB})$, causing the frequency of optimum S_{11} to shift towards frequencies lower than ω_{LO}. The total C_p is about 1 pF in this receiver design. Assuming that $R_s \gg R_{sw}$, the input impedance around ω_{LO} becomes:

$$R_{in}(\omega_{LO})||(j\omega_{LO}C_p)^{-1} = \frac{(R_{sh}(\omega_{LO})||\gamma 2R_{BB})(1 - j\omega_{LO}(R_{sh}(\omega_{LO})||\gamma 2R_{BB})C_p)}{1 + (\omega_{LO}(R_{sh}(\omega_{LO})||\gamma 2R_{BB})C_p)^2} \quad (15)$$

Note that this is not a purely resistive impedance, but also contains a negative imaginary part, degrading S_{11}. Apart from this (time invariant) capacitor C_p, the impedance of the BB capacitance is up-converted, resulting in a positive imaginary part for frequencies below ω_{LO}, but a negative inductance for frequencies above ω_{LO} [15]. This latter effect can cancel the imaginary part of Eqn. (15) at a frequency $\omega_{LO} - \Delta\omega$ that is also roughly the frequency of optimum S_{11} due to C_p. To bring the dip of S_{11} back to ω_{LO}, complex feedback with resistors R_{FIQ} can be applied [1]. The BB impedance jR_{FIQ}/A [15] is now up-converted with a scaling factor to cancel the term proportional to $-j(\omega_{LO}C_p)^{-1}$ in Eqn. (15). The required complex feedback resistance can be calculated as $R_{FIQ} = A/(2\gamma\omega_{LO}C_p)$ and lower resistance is demanded for the receiver operating at higher frequency. R_{FIQ} also introduces a real part making the BB admittance $Y_{BB} = (R_{BB})^{-1} = ((1 + A)/R_F + 1/R_{FIQ})$ is slightly higher (R_{BB} is lower). The C_p at RF input is in parallel with $R_{sh}(\omega_{LO})$ that is composed of all odd harmonic shunt impedances in the 4-path case. C_p decreases higher order harmonic shunt impedances and increases the folded noise. The $R_{sh}(\omega_{LO})$ for a 4-path mixer-first receiver can be approximated as [14]:

$$R_{sh}(\omega_{LO}) \approx 4.3R_{sw}(1 + (4R_{sw}C_p\omega_{LO} + R_{sw}/R_s)^{-1}) \quad (16)$$

At very low frequency $R_{sw} \approx 1.1\ \Omega$ (W/L of a NMOS switch is 300 um/40 nm), $C_p \approx 1$ pF yields $R_{sh}(0) = 4.3(R_s + R_{sw}) \approx 220\ \Omega$. At higher frequency that is $\omega_{LO} = 2$ GHz, $R_{sh}(\omega_{LO})$ is reduced to 68 Ω, causing lower $R_{in}(\omega_{LO}) = R_{sh}(\omega_{LO})||(\gamma 2R_{BB}) = 33\ \Omega$ and worse input matching. The RF input gain can be expressed as a voltage division of $V_sR_{in}(\omega_{LO})/(R_s + R_{in}(\omega_{LO}))$. The lower $R_{in}(\omega_{LO})$ due to C_p also causes gain loss and can be computed as:

$$\text{Gain loss @RF} = 20log[(\frac{R_{in}(\omega_{LO})}{R_s+R_{in}(\omega_{LO})})/(\frac{R_{in}(0)}{R_s+R_{in}(0)})] \quad (17)$$

For example, the RF gain loss is about 2 dB at 2-GHz LO frequency. To compensate the loss at RF, BB feedback resistance R_F can be adjusted to be higher to obtain higher up-converted resistance and bring the effective $R_{in}(\omega_{LO})$ to 50 Ω. Both S_{11} degradation and gain loss at higher LO frequency can be compensated by R_F tuning. Note that it can be well compensated when $R_{sh}(\omega_{LO}) > 50\ \Omega$. Unfortunately, the presence of C_p at the RF-input still increasing the harmonic folding noise although the gain loss and S_{11} are compensated.

V. MEASUREMENT RESULTS AND COMPARISON

This test chip has been fabricated in a Global Foundries 45nm Partially Depleted SOI technology. A 4x4 QFN package was used. The total area including pads and decoupling capacitors is 1300 umx1100 um while the active area is 0.8 mm^2. The highest aluminum layer covers almost the whole receiver chip to provide very strong ground shielding. Figure 11 shows the chip micrograph. The external differential clock is applied from the top side, while the RF input signal is applied from the bottom to minimize coupling. Wideband off-chip hybrids were used to serve as baluns to provide a differential RF signal and impedance match to the 100- Ω differential chip input. Both the hybrid and cable losses were de-embedded for all measurements.

A. S_{21} and S_{11}

Because the BB amplifier is not able to directly drive a 50-Ω load, a low noise external measurement buffer with differential high-impedance input and single-ended 50-Ω output impedance was adopted. A weak tone of −50 dBm is applied to the RF input and the BB output is observed to obtain the conversion gain. Figure 12 shows the measured and simulated gain and S_{11} as a function of the RF input frequency for a 2-GHz LO. The calculated transfer function from Eqn. (8) is also provided. Both BB negative feedback and the complex-feedback resistors are programmed to compensate RF gain loss and S_{11} shifting due to parasitic capacitance at the RF input. 21-dB gain and 20-MHz BPF channel bandwidth are obtained. As in simulation, the passband shows an asymmetrical slope induced by the complex feedback resistors. The peak of the gain roughly occurs at the middle between the center frequency and −3 dB frequency, where the magnitude of imaginary part of the input impedance is maximum. The jR_{FIQ}/A is up-converted to cancel the unwanted $-j(\omega_{\mathrm{LO}}C_{\mathrm{p}})^{-1}$ due to parasitic capacitance at the RF input, as discussed in section IV-E. However, the gain of the BB amplifier $A(s)$ is a function of frequency. Complete cancellation only happens at the exact center frequency. As the RF frequency changes, the residue $-j/(\omega_{\mathrm{LO}}C_{\mathrm{p}} - A/(2\gamma R_{\mathrm{FIQ}}))$ remains a negative imaginary impedance. The up-converted imaginary part of the BB impedance is positive for the low RF-side-band but negative for the upper sideband [15]. The combination of these imaginary impedances result in an asymmetrical impedance profile at the RF input port. Together with pass-band ripple, this slope in the gain can be compensated in the digital domain. The complex poles are located at BB frequency of 10 MHz. The measured filter roll-off is about 8.4 dB from 10 to 20 MHz offset frequency (It is 9.3 dB for an ideal Butterworth filter), 8.2 dB from 20 to 40 MHz offset frequency (It is 11.8 dB for an ideal Butterworth filter). The less steep filter shape is due to a zero at BB frequency of $(2\pi \cdot 0.5R_{\mathrm{a}}C_{\mathrm{a}})^{-1}$ =31 MHz that can be found in Eqn. (8).

B. B1dB, IIP2 and IIP3

To deal with a blocker that is close to the RX band is in general more difficult, as there are less octaves of filter suppression. Hence, it is preferable for fair benchmarking of linearity to consider the relative frequency offset normalized to the $f_{-3\mathrm{dB,BB}}$. Figure 13 shows the measured B1dB as a function of $\Delta f/f_{-3\mathrm{dB,BB}}$ for f_{LO}=2 GHz and a desired signal is at 2.001

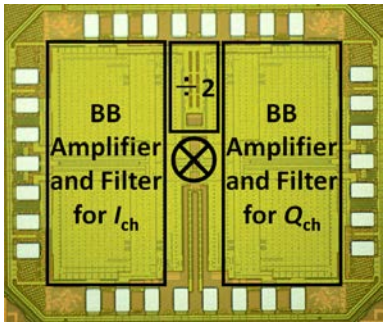

Fig. 11. Chip microphotograph.

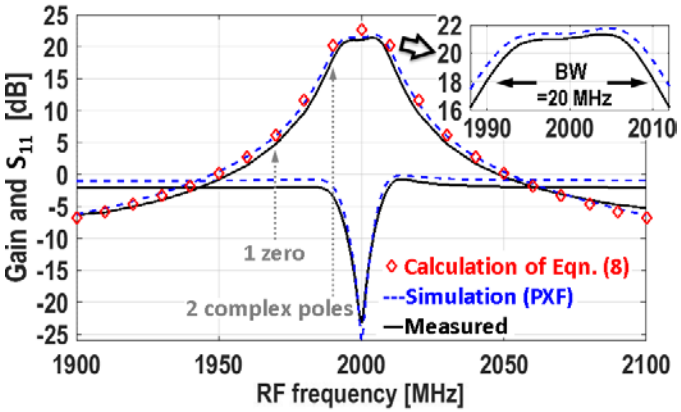

Fig. 12. Measured and simulated gain and S_{11} versus RF frequency (f_{LO}=2 GHz). The calculated transfer function from Eqn. (8) is also provided.

GHz (f_{BB}=1 MHz) for this work. Already at $\Delta f/f_{-3\mathrm{dB,BB}}$>2, B1dB is >0 dBm, while for $\Delta f/f_{-3\mathrm{dB,BB}}$>6, B1dB>+10 dBm. Note that this design only uses a 1.2-V supply (other designs like [5] artificially boost B1dB by increasing the supply voltage introducing device reliability concerns). The comparison with several blocker-tolerant receivers that achieved >+10-dBm B1dB [5, 10, 21] are also shown. A few dB improvement for maximum B1dB can be achieved by adopting complementary MOS switches [21] or using the bottom-plate mixing technique proposed in [10] to realize more constant switch resistance. It also can be extended by applying higher supply voltage [5] at the cost of higher power consumption. Interestingly, the B1dB is improved by complementary switches but not IIP3 and IIP2. The bias point of the source and drain of both the PMOS and NMOS of a complementary switch is about $VDD/2$ in [21]. For this complementary switch design, the overdrive voltage is smaller than the designs with only NMOS switches [1, 3, 11, 13]. As a result, the switch resistance is higher leading to worse IIP3 and IIP2 [14]. Thanks to the steeper filter roll-off due to the complex pole pair in our design, we achieve a higher B1dB at lower relative frequency offset as shown in Fig. 13.

IIP3 and IIP2 measurements are performed by two-tone tests. Circulators that offer higher than 20 dB isolation are applied between the two blocker signal generators to prevent intermodulation in the test setup, so that over +55-dBm IIP3 was achieved in the test setup itself. For LTE radio applications, the transmitter signal frequency is lower than the receiver frequency for most of the bands. Therefore, the test tones were chosen at $f_1 = f_{\mathrm{LO}} - \Delta f$ and $f_2 = f_{\mathrm{LO}} - 2\Delta f + 500$ kHz for IIP3 measurements, and at $f_1 = f_{\mathrm{LO}} - \Delta f$ and $f_2 = f_{\mathrm{LO}} - \Delta f + 500$ kHz for IIP2 measurements. This choice keeps the

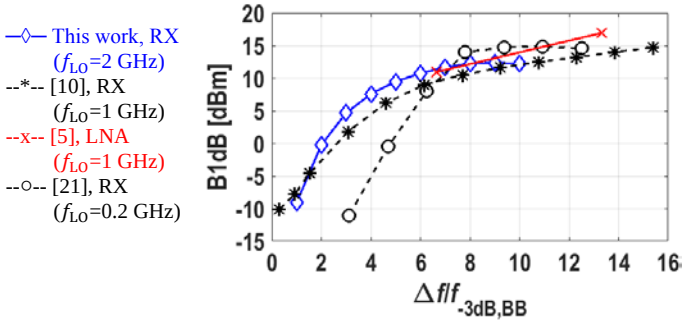

Fig. 13. Measured B1dB as a function of relative blocker frequency offset $\Delta f/f_{-3\mathrm{dB,BB}}$ and comparison with other blocker-tolerant RF front ends.

resulting IM3 or IM2 product at a constant BB frequency of 500 kHz. Measured IIP3 and IIP2 as a function of Δf for a 2-GHz LO are shown in Fig. 14. At Δf=80 MHz, very high IIP3 of +39 dBm and IIP2 of +88 dBm are achieved. Figure 15(a) shows the input referred IM3 as a function of the blocker power for a 2-GHz LO and Δf=80 MHz. The measured P_{IIM3} follows the extrapolation line up to an input power of 0 dBm and +39-dBm IIP3 is obtained.

C. NF and gain vs LO frequency

Measured gain as a function of LO frequency is shown in Fig. 15(b) and DSB NF is shown in Fig. 15(c). Measurement results show that the operating frequency can be up to 8 GHz, where an external clock $2f_{\mathrm{LO}}$=16 GHz is applied. The limitation is the achievable rising and falling time of the inverter buffers that drive the mixer switches. It is a process related parameter, where a more advanced technology achieves higher operating frequency. Measurement shows that the receiver gain is kept within 1-dB degradation up to f_{LO}=3 GHz. NF measurements were performed using the Y-factor method with an external noise source. It is below 3 dB up to f_{LO}=2 GHz. The input parasitic capacitance due to mixer switches, input tracks and pads is not taken into account in Eqn. (14) of section IV-D noise analysis. In the practical circuit, this lowers the impedance seen by the source voltage at higher RF frequencies. Therefore, the source resistance contributes a lower percentage of the total output noise at higher frequencies and NF increases. Also, lower complex feedback resistance is required to compensate for more S_{11} shifting at higher f_{LO} leading to more NF degradation (see also section IV-E).

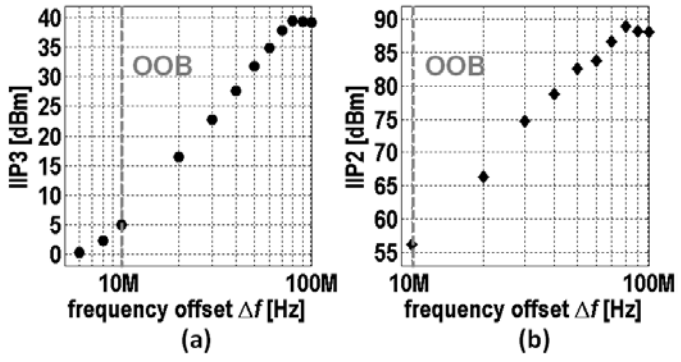

Fig. 14. Measured (a) IIP3 and (b) IIP2 versus blocker frequency offset Δf at f_{LO}=2 GHz.

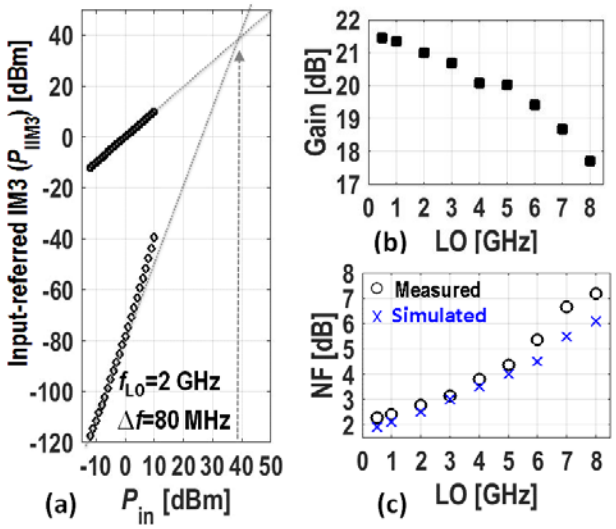

Fig. 15. (a) Measured P_{IIM3} versus P_{in} for Δf=80 MHz at f_{LO}=2 GHz, (b) measured gain and (c) DSB NF versus LO frequency. (PSS+PNOISE transistor-level simulated NF is also shown.)

D. Blocker NF

A divide-by-two frequency divider is employed. The 25-% duty cycle LO pulses for quadrature mixing are obtained by combining the divider output with AND logical gates [1, 22]. In order to cover RF-frequencies >6 GHz and achieve low phase noise, the 4-phase clock generator consumes 30 mW/GHz, targeting a phase noise of −171 dBc/Hz at 80-MHz offset frequency (=duplexer offset). To ensure very low in-band noise of the blocker signal generator and low phase noise of the LO clock generator, two external tunable narrow-band BPFs in cascade were applied to the output of the signal generators. This is done to ensure that the reciprocal mixing of the chip dominates performance, instead of phase noise from the measurement equipment. Figure 16 shows the measured NF as a function of blocker power for 1.4-GHz LO and blocker is 80-MHz from f_{LO}. Overall, the presence of strong blockers degrades NF due to reciprocal mixing and gain compression. Since the measured B1dB is high as +12 dBm, the blocker NF degradation is most likely due to reciprocal mixing. The measured desensitization is only 2.2 dB for a 0-dBm blocker, and 7.1 dB for a 8-dBm blocker. This design achieved a low 0-dBm blocker NF of 4.7 dB which is comparable to one of the best results published so far with a noise cancelling RX [17]. Note that, since an active g_{m} circuit is required at the RF input

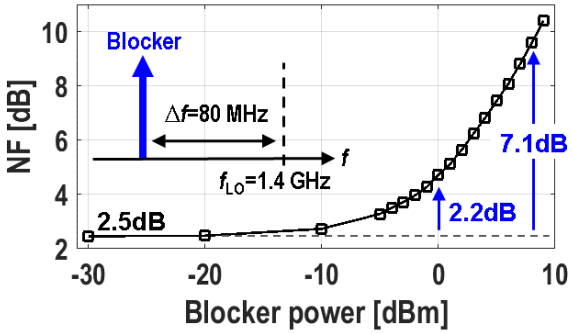

Fig. 16. Measured blocker NF for f_{LO}=1.4 GHz. (The highest f_{LO} for blocker NF measurement is 1.4 GHz due to the availability of external bandpass filters for blocker and clock sources.)

port for noise cancelling, linearity is limited in [17]. As a result, the achieved B1dB is <0 dBm which causes blocker NF to degrade rapidly with higher blocker power (>10-dB NF for +3-dBm blocker). Thanks to the steeper filter roll-off due to complex poles at the RF input that reject blockers, this design maintains a blocker NF<+10 dB up to an +8-dBm blocker.

E. Performance comparison

Figure 17 shows an IIP3 benchmark of blocker-tolerant RF front ends as a function of $\Delta f/f_{-3\text{dB,BB}}$. Circuit type, NF, and operating frequency are also indicated. This design achieves high linearity while keeping NF <3 dB. Note that the RX design in [10] which is also proposed by us achieved higher linearity but limited operating frequency and significantly higher NF. A performance summary and comparison is shown in the TABLE II. Compared to prior art, the receiver achieves high IIP3, IIP2 and wider operating frequency f_{RF}, while maintaining comparable NF and power consumption. This confirms the effectiveness of the higher RF BPF selectivity provided by the proposed mixer-first receiver exploiting positive capacitive feedback.

F. LTE band 5 diversity antenna path experiment

Figure 18 shows a test setup used to evaluate the sensitivity for a LTE band 5 scenario. The TX frequency is 824-849 MHz, and the RX frequency is 869-894 MHz, i.e. 45 MHz duplex spacing. An in-band signal at the RX band (880 MHz) plus 1.7 MHz offset is applied to the RX port of the triplexer. A 20-MHz BW modulated signal is applied at 835 MHz to the TX port, and a CW blocker is applied to BLK port at 790 MHz. The triplexer implements bandpass filtering and combines the three signals and the sum is connected to the main antenna of an actual cell phone antenna via an SMA connector. There is about 15 dB isolation between the main and diversity antennas. The diversity antenna path of this cell phone is connected to this receiver chip for a sensitivity test. Assuming the noise floor is *KT* at the antenna, the NF is obtained by observing the SNR degradation at the receiver output. The external measurement buffer amplifier was used again, and a LPF filter is added at the external buffer output to prevent the corruption of the spectrum analyzer performance due to strong down-converted TX signals. The hybrid and cable loss as well as the external buffer and spectrum analyzer noise were de-embedded. Figure 19 shows the measured RX NF as a function of TX power. The measured NF is about 4.7 dB at very low TX power while the measured NF using the Y-factor method in Fig. 15(c) is about 2.5 dB. This is because the antenna only provides the RX with an in-band 50-Ω impedance matching, while there is wideband 50-Ω impedance for the external noise source used in the Y-factor NF-measurement. The lower harmonic shunt impedance generates more noise current bringing, leading to higher NF. First, we measured the NF when the TX modulation is off and the TX produces a single tone at 835 MHz. This corresponds to a blocker NF measurement. The measured desensitization is only 0.7 dB for a 15-dBm blocker and 4.4 dB for 24-dBm blocker. Next, the TX modulation is turned-on and the IM2 increases the noise floor. The measured desensitization due to IM2 and reciprocal mixing is about 3 dB when the TX power is +15 dBm. If the TX power is higher than +25 dBm, the NF deteriorates rapidly since the TX leakage power to diversity RX is higher than B1dB and gain compression worsens the NF as well. A −15 dBm CW blocker at 790 MHz is also fed to the BLK port for IIP3 desensitization tests. Since there is about 15 dB isolation, the actual CW blocker at the diversity RX is about −30 dBm. The noise floor induced by IM3 in a certain BW can be calculated as $N_{\text{IM3}} = 3P_{\text{in}} - 2 \cdot IIP3 - 10log(\text{BW})$. The IIP3 is about +30 dBm at 45-MHz duplexer frequency in this design. For a P_{in} =− 30 dBm, BB BW of 10 MHz, N_{IM3} is about −220 dBm which is much lower than *KT*, therefore the IIP3 induced desensitization was not detectable.

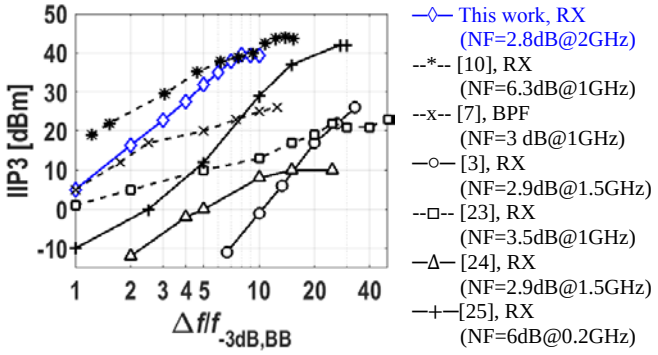

Fig. 17. The IIP3 benchmark of blocker-tolerant RF front ends as a function of $\Delta f/f_{-3\text{dB,BB}}$.

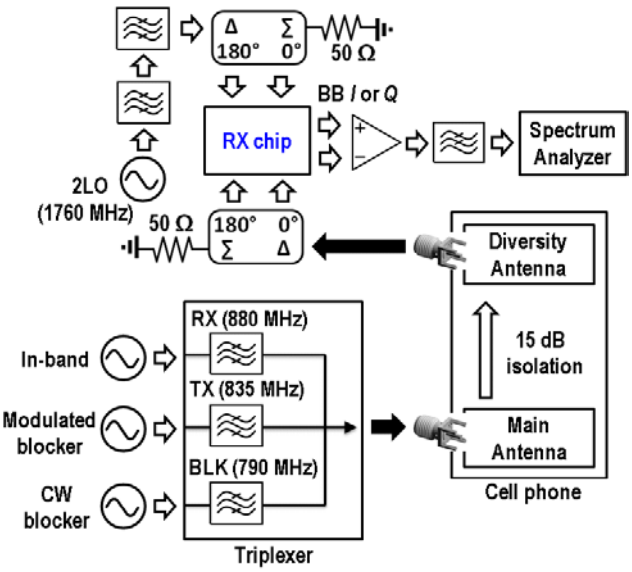

Fig. 18. LTE band 5 sensitivity test setup.

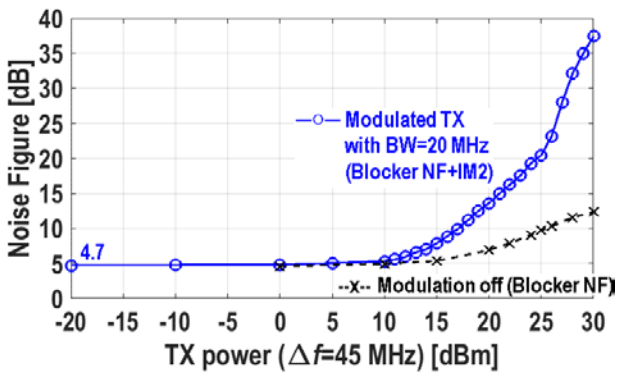

Fig. 19. Measured diversity receiver NF as a function of TX power.

TABLE II
RESULT SUMMARY AND COMPARISON WITH PRIOR ARTS

	*JSSC*10[1]	*JSSC*12[17]	*JSSC*13[7]	*JSSC*15[9]	*RFIC*15[2]	*RFIC*15[3]	*RFIC*15[5]	*ISSCC*17[10]	This Work
Architecture	Mixer first	Mixer first with Noise Cancelling	N-path filter	Mixer first +2nd order baseband	Mixer first with LO leakage suppression	Mixer first with positive resistive feedback	Feedback with N-path filter	N-path filters with bottom -plate mixing	Mixer first with positive capacitive feedback
Circuit type	Receiver	Receiver	LNA/Filter	Receiver	Receiver	Receiver	LNA/Filter	Receiver	Receiver
Technology	65nm	40nm	65nm	65nm	28nm	65nm	32nm SOI	28nm	45nm SOI
f_{RF}[GHz]	0.1-2.4	0.08-2.7	0.1-1.2	0.5-3	0.4-3.5	0.7-3.8	0.4-6	0.1-2.0	0.2-8
Gain[dB]	40-70	72	25	50	35	40	12	16	21
BB BW[MHz]	10	2	4	1-30	15-50	3	7.5	6.5	10
OOB IIP3[dBm]	25 $\Delta f/BW$ =10	13.5 $\Delta f/BW$ =40	26 $\Delta f/BW$ =12.5	−4.8 $\Delta f/BW$ =8	20.5 $\Delta f/BW$ =3.3	26 $\Delta f/BW$ =33.3	36 $\Delta f/BW$ =6.7	44 $\Delta f/BW$ =12.3	39 $\Delta f/BW$ =8
OOB IIP2[dBm]	56	55	NA	NA	64	65	NA	90	88
B1dB[dBm]	10 $\Delta f/BW$ =10	−2 $\Delta f/BW$ =40	7 $\Delta f/BW$ =12.5	−10 $\Delta f/BW$ =8	4.6 $\Delta f/BW$ =3.3	3 $\Delta f/BW$ =33.3	>17 $\Delta f/BW$ =13.3	13 $\Delta f/BW$ =12.3	12 $\Delta f/BW$ =8
NF[dB]	4±1	1.9 (2GHz f_{LO})	2.8	3.8-4.7	2.4-2.6	2.5-4.5	3.6-4.9	6.3 (1GHz f_{LO})	2.3-5.4 (0.5-6GHz f_{LO})
0dBm Blocker NF[dB]	NA	4.1 (f_{LO}=1.5GHz)	NA	NA	6.5 (f_{LO}=2GHz)	NA	NA	8.1 (f_{LO}=1.3GHz)	4.7 (f_{LO}=1.4GHz)
LO leakage [dBm]	−65 (f_{LO}=1GHz)	NA	<−64 (f_{LO}=1GHz)	NA	<−62	<−60	<−40	NA	<−65
Supply[V]	1.2/2.5	1.2/2.5	1.2	1.2/2.5	1/1.5	1.2	2	1.2/1.0	1.2
Power[mW]	37-70	27-60	15-48	RX:76-168 LO:54-194	38-75	27-75	81-209	38-96	50mW*+ 30mW/GHz**
Area[mm^2]	2.5	1.2	0.27	7.8	0.23	0.23	0.28	0.49	0.8

***power consumption of BB amplifiers = 50 mW, **clock generator power is 30 mW/GHz.**

VI. CONCLUSION

In this paper, a mixer-first receiver with enhanced selectivity due to capacitive positive feedback was proposed. It improves the filter shape exploiting a complex pole pair, while achieving sub-3 dB noise figure and high linearity (IIP3>36 dBm, B1dB>10 dBm) as required for LTE FDD diversity receivers. Important receiver properties were analyzed, like filter shape in terms of natural frequency ω_0, quality factor Q, bandwidth and noise figure. To evaluate stability, the loop gain as a function of frequency was related to the amplifier gain, attenuator transfer and the capacitor ratio of two feedback paths. Loop gain is reliably kept below −6 dB and the loop stability is insensitive to PVT and antenna impedance variations. This receiver design covers all sub-6GHz cellular bands and achieves a high IIP3 of +39 dBm, IIP2 of +88 dBm and blocker 1dB gain compression point of +12 dBm for a blocker frequency offset of 80 MHz at 2-GHz LO while achieving a NF of 2.8 dB. The measured NF ranges from 2.4 dB at f_{LO}=1 GHz to 5.4 dB at f_{LO}=6 GHz. The measured desensitization is only 2.2 dB for 0-dBm blocker, and 7.1 dB for 8-dBm blocker, demonstrating robustness to TX leakage and strong blockers.

ACKNOWLEDGMENT

The authors would like to thank Gerard Wienk for CAD assistance and Henk de Vries for help during measurements. The authors also thank GlobalFoundries for supporting the chip fabrication.

REFERENCES

[1] C. Andrews, and A. C. Molnar, "A Passive Mixer-First Receiver With Digitally Controlled and Widely Tunable RF Interface," *IEEE J. Solid State Circuits*, vol. 45, NO. 12, pp. 2696-2708, Dec. 2010.

[2] C. Wu, Y. Wang, B. Nikolic, C. Hull, "A Passive-Mixer-First Receiver with LO Leakage Suppression, 2.6dB NF, >15dBm Wide-Band IIP3, 66dB IRR Supporting Non-contiguous Carrier Aggregation," *IEEE Radio Frequency Integrated Circuits Symp*., pp. 155–158, June 2015.

[3] A. Nejdel *et al*., "A Positive Feedback Passive Mixer-First Receiver Front-End," *IEEE Radio Frequency Integrated Circuits Symp*., pp. 79–82, June 2015.

[4] V. Aparin and L. Larson, "Analysis and reduction of cross-modulation distortion in CDMA receivers," *IEEE Trans. Microw. Theory Techn*., vol. 51, no. 5, pp. 1591–1602, May 2003.

[5] C. Luo, P. S. Gudem, J. F. Buckwalter, "0.4-6 GHz,17-dBm B1dB, 36-dBm IIP3 Channel-selecting, Low-noise Amplifier for SAW-less 3G/4G FDD Receivers," *IEEE Radio Frequency Integrated Circuits Symp*., pp. 299–302, June 2015.

[6] A. Ghaffari, E. A. M. Klumperink, M. C. M. Soer, and B. Nauta, "Tunable High-Q N-Path Band-Pass Filters: Modeling and Verification," *IEEE J. Solid State Circuits*, vol. 46, NO. 5, pp. 998-1010, MAY 2011.

[7] M. Darvishi, R. van der Zee, and B. Nauta, " Design of Active N-Path Filters, " *IEEE J. Solid State Circuits*, vol. 48, NO. 12, pp. 2962-2976, Dec. 2013.

[8] H. K. Subramaniyan, E. A. M. Klumperink, V. Srinivasan, A. Kiaei, and B. Nauta, " RF Transconductor Linearization Robust to Process, Voltage and Temperature Variations," *IEEE J. Solid State Circuits*, vol. 50, NO. 11, pp. 2591-2602, Nov. 2015.

[9] R. Chen, and H. Hashemi,, "Dual-Carrier Aggregation Receiver With Reconfigurable Front-End RF Signal Conditioning," *IEEE J. Solid State Circuits*, vol. 50, NO. 8, pp. 1874-1888, Aug. 2015.

[10] Y. Lien, E. Klumperink, B. Tenbroek, J. Strange, B. Nauta, "A High-Linearity CMOS Receiver Achieving +44dBm IIP3 and +13dBm B_{1dB}

for SAW-Less LTE Radio," *IEEE ISSCC Dig. Tech Papers*, pp. 412-413, Feb. 2017.

[11] Y. Lien, E. Klumperink, B. Tenbroek, J. Strange, B. Nauta, "A Mixer-First Receiver with Enhanced Selectivity by Capacitive Positive Feedback Achieving +39dBm IIP3 and <3dB Noise Figure for SAW-Less LTE Radio," *IEEE Radio Frequency Integrated Circuits Symp*., pp. 280–283, June 2017.

[12] E. A. M. Klumperink, H. J. Westerveld and B. Nauta, "N-path filters and mixer-first receivers: A review," 2017 *IEEE Custom Integrated Circuits Conference* (*CICC*), Austin, TX, USA, 2017, pp. 1-8.

[13] M. Soer, E. Klumperink, Z. Ru, F. van Vliet, and B. Nauta, "A 0.2-to-2.0 GHz 65 nm CMOS receiver without LNA achieving 11 dBm IIP3 and 6.5 dB NF," in *IEEE ISSCC Dig. Tech Papers*, pp. 222–223, 223a, Feb. 2009.

[14] D. Yang, C. Andrews, and A. Molnar, "Optimized Design of N-Phase Passive Mixer-First Receivers in Wideband Operation," *IEEE Trans. Circuits Syst. I*, vol. 62, no. 11, pp. 2759–2769, 2015.

[15] C. Andrews, and A. C. Molnar, "Implications of Passive Mixer Transparency for Impedance Matching and Noise Figure in Passive Mixer-First Receivers," *IEEE Trans. Circuits Syst. I*, vol. 57, no. 12, pp. 3092–3103, 2010.

[16] B. Nauta, " A CMOS Transconductance-C Filter Technique for Very High Frequencies," *IEEE J. Solid State Circuits*, vol. 27, NO. 2, pp. 142-153, Feb. 1992.

[17] D. Murphy et al., "A Blocker-Tolerant, Noise-Cancelling Receiver Suitable for Wideband Wireless Applications," *IEEE J. Solid State Circuits*, vol. 47, NO. 12, pp. 2943-2963, Dec. 2012.

[18] S . Krishnan, J. G, Fossum, P. C. Yeh, O. Faynot, S. Cristoloveanu, and J. Gautie, "Floating-Body Kinks and Dynamic Effects in Fully Depleted SOI MOSFETs," in *IEEE International SOI Conference*, Oct. 1995, pp. 10–11.

[19] K. R. Boyle, Y. Yuan, and L. P. Ligthart,,"Analysis of Mobile Phone Antenna Impedance Variations With User Proximity," *IEEE TRANSACTIONS ON ANTENNAS AND PROPAGATION. I*, vol. 55, no. 2, pp. 364–372, 2007.

[20] Willy Sansen, "Distortion in Elementary Transistor Circuits," *IEEE Trans. Circuits Syst. II*, vol. 57, no. 6, pp. 315–325, 1999.

[21] A. Yang Xu, and Peter R. Kinget, "A Switched-Capacitor RF Front End With Embedded Programmable High-Order Filtering," *IEEE J. Solid State Circuits*, vol. 51, NO. 5, pp. 1154-1167, MAY 2016.

[22] A. Mirzaei, H. Darabi, J. C. Leete, and Y. Chang, "Analysis and Optimization of Direct-Conversion Receivers With 25% Duty-Cycle Current-Driven Passive Mixers," *IEEE Trans. Circuits Syst. I*, vol. 57, no. 9, pp. 2353–2366, Sep. 2010.

[23] H. Hedayati, V. A., K. Entesari, "A +22dBm IIP3 and 3.5dB NF Wideband Receiver with RF and Baseband Blocker Filtering Techniques," *IEEE Symp. On VLSI Circuit*, pp. 36-37, Jun. 2014.

[24] Z. Lin, P. Mak1, R. P. Martins, " A 0.028mm^2 11mW Single-Mixing Blocker-Tolerant Receiver with Double-RF N-Path Filtering, S_{11} Centering, +13dBm OB-IIP3 and 1.5-to-2.9dB NF," *IEEE ISSCC Dig. Tech Papers*, pp. 36-37, Feb. 2015.

[25] H. Westerveld, E. Klumperink, B. Nauta, " A Cross-Coupled Switch-RC Mixer-First Technique achieving +41dBm Out-of-Band IIP3," *IEEE Radio Frequency Integrated Circuits Symp*., pp. 246–249, June 2016.